Rb deposition on alkanethiolate monolayers on Au

Cite as: J. Appl. Phys. **112**, 023110 (2012); https://doi.org/10.1063/1.4739736
Submitted: 03 May 2012 . Accepted: 27 June 2012 . Published Online: 24 July 2012

A. M. Hibberd, R. M. Thorman, J. D. Wnuk, and S. L. Bernasek

Rb deposition on alkanethiolate monolayers on Au

A. M. Hibberd, R. M. Thorman, J. D. Wnuk, and S. L. Bernasek
Department of Chemistry, Princeton University, Princeton, New Jersey 08544, USA

(Received 3 May 2012; accepted 27 June 2012; published online 24 July 2012)

The performance of many devices utilizing alkali metal (AM) atoms is dependent upon properties of organic thin films used to line the inner walls of the glass vessel in which the system is contained. In this study, two alkanethiolate self-assembled monolayers on Au, 1-dodecanethiolate and 1-octanethiolate, are employed as model systems to investigate alkali metal atom-thin film interactions. Before and after Rb deposition, the alkanethiolate surface is analyzed with x-ray photoelectron spectroscopy (XPS), including angle-resolved XPS and XPS with an applied dc bias. Following Rb deposition, a shift of the C1s core-level to higher binding energy was observed; additionally, with continued Rb deposition, the atomic percent of Rb on the surface was found to saturate. The importance of these observations with regard to atomic magnetometers and the light induced atomic desorption effect are discussed. © *2012 American Institute of Physics*. [http://dx.doi.org/10.1063/1.4739736]

INTRODUCTION

Due to the ease of manipulation of the single valence electron, alkali metal (AM) atoms are used in numerous technological applications and tests of fundamental physics. For example, spin polarized AM atoms are used in atomic magnetometers,[1] atomic clocks,[2] squeezed spin state experiments,[3] and for quantum memory.[4] The performance of devices utilizing AM atoms is often dictated by microscopic interactions occurring between AM atoms and organic thin films used to line the inner walls of the glass vessel (referred to as atomic vapor cells) in which the system is contained. For example, atomic magnetometers, devices used for sensitive measurements of magnetic fields, typically use cell surfaces coated with paraffin wax[1,5,6] to preserve the orientation of spin-polarized AM atoms; long spin polarization times are necessary as these lifetimes govern the ultimate sensitivity and precision of such devices.[7] Due to a higher thermal stability than paraffins,[8,9] certain siloxane films have also been investigated for use in atomic magnetometer vapor cells.[10–13]

In addition to suppressing spin relaxation, vapor cell organic wall coatings that are "cured" can be used as a source of AM atoms for the loading of chip-scale atom traps[14] and Bose-Einstein condensates.[15] A coated atomic vapor cell containing an AM atom source (a solid droplet of the metal) that is heated for an extended period of time reaches a cured state as evaporated AM atoms are absorbed into the coating and adsorb on the surface.[8,16,17] Not until a cell is cured can stable atomic vapor pressures within the cell be maintained. AM atoms retained in/on the coating (typically paraffins or siloxanes) may be desorbed and ejected into the cell interior using a desorbing light source;[7,18–23] this effect is referred to as light induced atomic desorption (LIAD) and allows for rapid increase in atomic vapor densities within the cell, greater than can be achieved thermally.[24] The effectiveness of atomic magnetometer coatings, as well as the efficiency of LIAD, is highly dependent on thin film properties. For example, the two widely used coatings, paraffin wax and octadecyltrichlorosilane (OTS), lead to spin polarization lifetimes in atomic vapor cells that differ by orders of magnitude.[8,12,21,25,26] If it is the surface structure that governs coating performance,[8,27] the variability between paraffin and OTS, both terminating as long-chain hydrocarbons, is not easily understood. Moreover, even among cells coated with the same material and produced under identical conditions, polarization lifetimes are found to be non-reproducible.[28,29] As another example, among a collection of coated cells prepared for LIAD efficiency measurements, variability was found despite the fact that all coatings were long-chain hydrocarbons.[30] The physical and chemical interactions that occur between AM atoms and coatings that suppress spin relaxation, lead to the eventual loss of polarization, and take place during LIAD, remain largely unknown. Additionally, the ability to rationalize observations of coating performance is hindered by a lack of knowledge of the microscopic interactions occurring between AM atoms and vapor cell coatings.

This study examines AM atom-organic thin film interactions in order to broaden understanding of the microscopic processes occurring in atomic vapor cells that may play a role in spin relaxation and LIAD. Arguably, the poor molecular ordering of commonly used coatings on cell walls inhibits clear identification of critical film properties. Thus, in this report, alkanethiolate monolayers on Au,[31,32] a widely studied class of self-assembled monolayers (SAMs), are employed as model films. SAMs are nano-scaled films formed by the covalent attachment of a headgroup to an underlying substrate; in particular, alkylthiols ($CH_3(CH_2)_n$–SH) anchor to Au substrates through thiolate (R–S–Au) bonds in the formation of alkanethiolate SAMs. SAMs are characterized as well-ordered and densely packed structures,[33] and as such, alkanethiolate monolayers are expected to provide a controlled system in which to probe the key interactions occurring between AM atoms and organic wall coatings.

Two alkanethiolate films, derived from 1-octanethiol ($CH_3(CH_2)_7$–SH) (OT) and 1-dodecanethiol ($CH_3(CH_2)_{11}$–SH) (DT) were examined. The films were exposed to atomic Rb

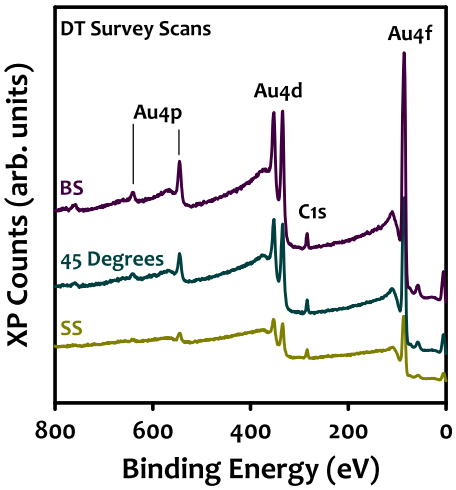

FIG. 1. Shown are survey spectra of 1-dodecanethiolate (DT) monolayers on Au at three collection angles (30°—SS, 45°, and 60°—BS). As expected, all signal intensities decrease and C1s core-level signals, relative to any one of the Au signals, increase as the take-off angle is changed from more BS to more SS. Sulfur peaks are not visible in the low resolution scans.

vapor and analyzed using x-ray photoelectron spectroscopy (XPS) and angle-resolved XPS (AR-XPS) before and after Rb deposition. In some cases, an external dc voltage bias was applied to the sample during XPS analysis. XPS quantitatively determines elemental compositions and identifies the chemical states of species present in the sample. AR-XPS is used to map out the location and state of elements as a function of depth. Applying an external bias to the sample during XPS analysis can detect differential charging and characterize electrical properties of the film.[34–36] Two films of varying chain length were chosen to probe effects that may arise due to changes in thickness; however, our experiments did not reveal any significant differences in results between OT and DT.

EXPERIMENTAL METHODS

Preparation of alkanethiolate monolayers on Au

Alkanethiolate SAMs were prepared in a manner similar to that published by Gorham *et al.*[37] Gold substrates (either gold foil or gold evaporated on a Cr/Si support) were diced into $\sim 1\,cm^2$ pieces and sonicated in ethanol (5 min), followed by hexanes (5 min), and dried under a flow of N_2. The Au substrates were cleaned via sputtering with Ar^+ for 15 min in an ultra-high vacuum (UHV) chamber (base pressure was $\sim 10^{-9}$ Torr). A PHI 04-303 ion gun was operated with a 2 keV acceleration voltage, 15 mA emission current, and 15 mPa Ar^+ pressure, with a rastering beam and target current of 1.8 μA. Removal of all surface contamination was verified with XPS. Following ion sputtering, the substrates were removed from the UHV chamber and immediately immersed in an alkylthiol in ethanol solution (~6–9 mM). After treatment in the solution overnight, the coated substrates were removed, rinsed sequentially with ethanol, hexanes, and Millipore DI H_2O (18 MΩ), and dried under a flow of Ar or N_2. Immediately following, the samples were introduced into the UHV chamber for XPS analysis and Rb deposition.

Rb atoms were deposited on the monolayer surface using a resistively heated AM atom dispenser (SAES Getters Group; Italy). Rb deposition occurred free of contamination as verified by the absence of impurity peaks in XPS wide-range scans. The dispenser was positioned directly above coated substrates in the XP spectrometer sample introduction chamber. Valves and vacuum lines allowed the dispenser to be isolated from samples and atmospheric contamination as needed, and this arrangement was used to inhibit oxidation of Rb after deposition on the sample surface. The dispenser was typically run for a few minutes at ~9 A for each deposition event. These settings resulted in significant Rb coverage as indicated by calculated atomic percents (*videas infra*). It should be noted that due to slight experimental variations (e.g., electrical contacts, power fluctuations, dispenser lifetimes, etc.) an absolute value of Rb coverage on the films cannot be determined.

SAM characterization

Contact angle goniometry was carried out by placing a sessile drop of H_2O on the film surface and measuring the resultant angle made between the surface and water drop with a Theta Optical Tensiometer (KSV Instruments; Finland) under ambient conditions. XPS spectra were collected on either a VG Scientific ESCALAB2 commercial instrument (Mg $K\alpha$ radiation; $h\upsilon = 1253.6$ eV), or a high resolution instrument employing monochromatic Al $K\alpha$ radiation ($h\upsilon = 1486.7$ eV) and a SPECS Phoibos 150 hemispherical

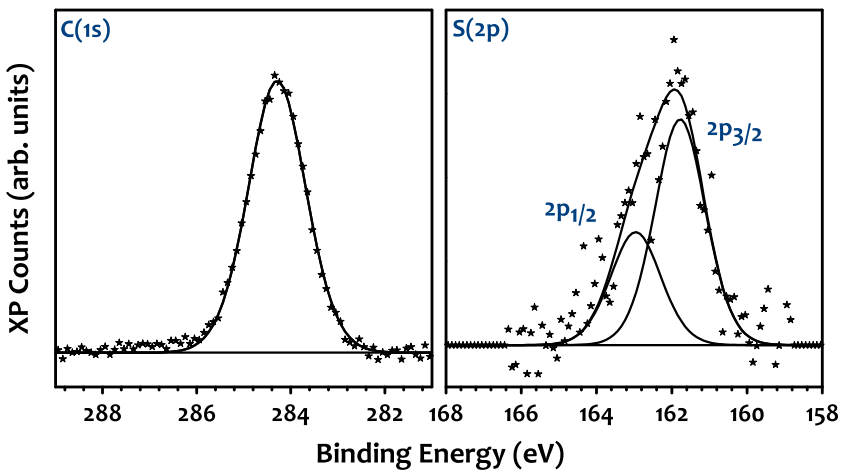

FIG. 2. High-resolution scans of the C1s and S2p regions for a 1-dodecanethiolate (DT) monolayer on Au.

energy analyzer. XPS survey scans were typically acquired at a 1 eV step size, 100 eV pass energy, and 1 ms dwell time, while higher resolution scans of the C1s, S2p, and Rb3d regions used a 0.5 eV step size, 20 eV pass energy, and 1 ms dwell time with 10–20 scans (>40 scans were required for S2p signals). Curve fitting of the core-level XPS lines was carried out with CASAXPS software using a nonlinear Shirley background subtraction and Gaussian–Lorentzian product function. The Au $4f_{7/2}$ signal at 84.0 eV was used for binding energy calibrations, and integrated peak intensities were corrected by element specific atomic sensitivity factors. Atomic percents were calculated by division of the integrated peak area of an element by the sum of the integrated peak areas of carbon, sulfur, and rubidium.

AR-XPS depth-profiling and XPS dc bias studies were performed in the SPECS system. Photoelectron take-off angles of 30°, 45°, and 60° (as defined from the surface plane), corresponding to surface sensitive (SS), average, and bulk sensitive (BS) scans, respectively, were used to acquire depth-dependent XP signals. An external bias was applied to the sample surface during XPS data acquisition using a dc power supply. These experiments were carried out at an applied bias of ±0.5, 1.0, 2.0, 5.0, and 15.0 V.

RESULTS AND DISCUSSION

The measured water contact angles of freshly prepared OT and DT SAMs were found to be 104.2° and 109.2°, respectively. These values are close to previously reported values and indicate a complete and densely packed monolayer formation.[38] XPS survey spectra of DT at three collection angles (30°—SS, 45°, and 60°—BS) are shown in Figure 1 (OT survey scans are equivalent). As can be seen by comparison of the spectra, as the surface sensitivity increases, and less photoelectrons escape the film, all peak intensities are attenuated. Close inspection indicates that the ratio of intensities of the C1s signal to any one of the Au signals increases going from BS to SS, as expected. Note that

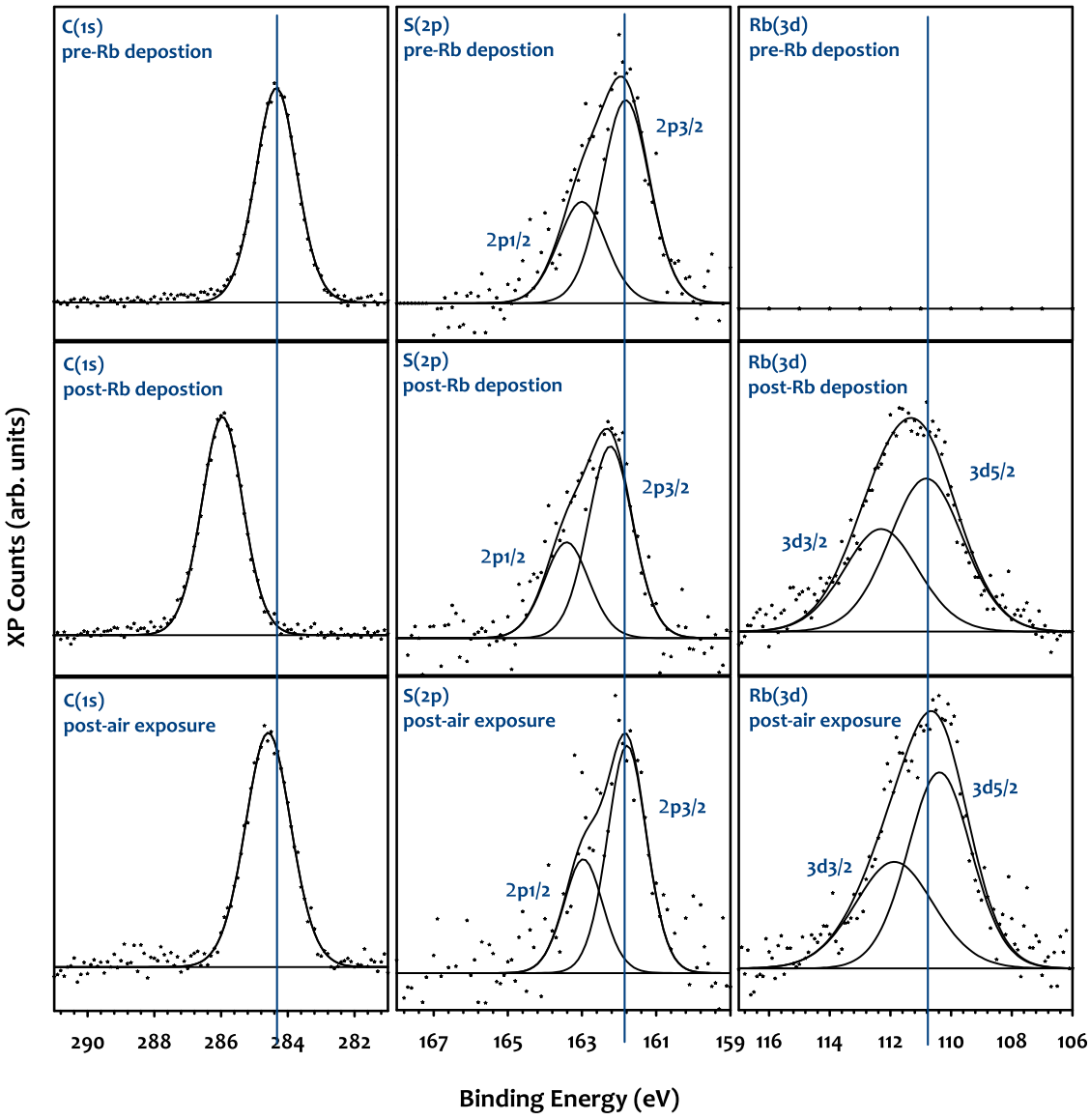

FIG. 3. Shown are the Rb3d, S2p, and C1s core-level signals of a dodecanethiolate (DT) monolayer on Au prior to Rb deposition (top panel), following a 2.5 min period of Rb deposition (middle panel), and after Rb oxidation (from exposure to air; bottom panel).

S2p peaks are not visible in the low resolution survey scans. High-resolution scans of the S2p and C1s regions for DT are shown in Figure 2 (OT scans are equivalent).

Following deposition of Rb on the DT surface, the atomic percent of Rb was found to be ~15% in the SS, 45°, and BS data sets. Similarly, the atomic percent of Rb in the 45° scan for OT was ~15%. This indicates that Rb atoms are able to intercalate into the film and that there is a fairly homogeneous distribution of Rb throughout the XPS sampling depth. Given an intermolecular chain separation on the order of ~4.5–5.0 Å as seen for alkanethiolates on polycrystalline Au,[33] it is not surprising that Rb atoms are observed to penetrate into the film (the Rb metallic radius is 248 pm). Based on this, and considering interchain distance in crystalline paraffin is ~4.7 Å,[39] it is expected that Rb atoms (and the smaller potassium) will easily diffuse into defects in poorly ordered paraffin and siloxane films. With regard to atomic magnetometers, this finding is significant as a polarized atom will lose its coherence with the spin ensemble as it is lost to the coating interior. This observation is also helpful in understanding the LIAD effect, as Rb distributed throughout the organic film can serve as the source of Rb atoms that are desorbed with light.

High-resolution XPS spectra of the Rb3d, S2p, and C1s regions of the DT SAM before and after Rb deposition are shown in Figure 3. Prior to Rb deposition, C1s and S2p core-level signals appear at expected binding energies of 284.4 eV and 161.8 eV, respectively. Following Rb deposition (deposition time ~2.5 min), a shift of the carbon signal to higher binding energy (286.0 eV) is observed; the sulfur signal also shifts, but to a lesser extent (162.2 eV). Shifts of the C1s signal to higher binding energy following Rb deposition are observed among all samples and at all collection angles. To observe the effects of Rb oxidation, the sample was removed from the vacuum chamber and exposed to ambient conditions for ~5 min. Following exposure to air, XPS analysis shows that the Rb3d peaks narrow and move to a lower binding energy in accord with AM atom oxidation.[40,41] Of note, C1s and S2p signals return to, or close to, pre-Rb deposition positions at 284.6 eV and 161.8 eV, respectively, after exposure to air.

Similar to the DT sample, OT C1s core-level signals in the OT sample shift to higher binding energy following Rb deposition. Shown in Table I are C1s, S2p, and Rb3d binding energies for the OT spectra before Rb deposition and after five Rb deposition steps (for each step deposition time was 1 min). The greatest change in C1s binding energy is observed after the first 1-min Rb deposition step (284.0 eV → 285.7 eV; $\Delta E = 1.7$ eV); by the 4-min deposition time the binding energy has reached a maximum value (286.1 eV) at 2.1 eV above the initial position (284.0 eV). The S2p signal shifts, but again, to a much lesser extent than the C1s signal, with the final position only 0.1 eV higher than the initial, pre-Rb, peak position. The Rb signal increases slightly during deposition until a maximum value of ~111.1 eV is reached. Alkali metal atom binding energies are known to be coverage dependent,[42–44] with shifts to higher binding observed at greater than monolayer coverages.[45] A similar analysis of the DT C1s data is presented as a plot of C1s binding energies vs. Rb deposition time (total deposition time was 40 min) in Figure 4. Again, the C1s binding energy rapidly increases at first and reaches a maximum position (~286.1 eV) that stays constant over the remaining deposition time.

The origin of the shift of the C1s signal to higher binding energy following exposure of the alkanethiolate SAMs to atomic Rb is not immediately obvious. As the formation of an electron-rich carbide species is known to result in a lower binding energy signal,[46–48] the chemical state of the carbon atoms in the Rb-alkanethiolate samples requires an alternate assignment. An important question that must be asked is whether the observed shifts are the result of charging. Surface charging can arise if the positive charge created by the ionization of atoms during XPS is not sufficiently neutralized; this can happen, for instance, if a sample is insulated. In our case, it is unlikely that the shifts are caused by charging as the films are on conducting substrates and no unexpected chemical shifts were observed in the samples prior to Rb deposition. Nevertheless, to verify that no charging was taking place, and to characterize electrical properties of our system, an external dc bias was applied to a Rb-DT sample during XPS analysis.[35,36] The data from the ±5.0 V bias study are presented in Figure 5. All potentials (±0.5, ±1.0, ±2.0, and ±15.0 V) gave analogous results. For all regions,

TABLE I. C1s, S2p, and Rb3d binding energies for a 1-octanethiolate (OT) monolayer on Au before Rb deposition and after five 1 min Rb deposition steps. Following Rb deposition, C1s signals shift to higher binding energy, with an initially large increase that levels off at the 4-min deposition time. S2p signals shift to a lesser extent, while Rb3d binding energies increase.

Rb deposition time (min)	C(1s) binding energy (eV)	S(2p) binding energy (eV)	Rb(3d) binding energy (eV)
0	284.0	162.1	…
1	285.7	161.9	110.6
2	285.9	161.9	110.8
3	286.0	162.2	111.0
4	286.1	162.3	111.1
5	286.1	162.2	111.1

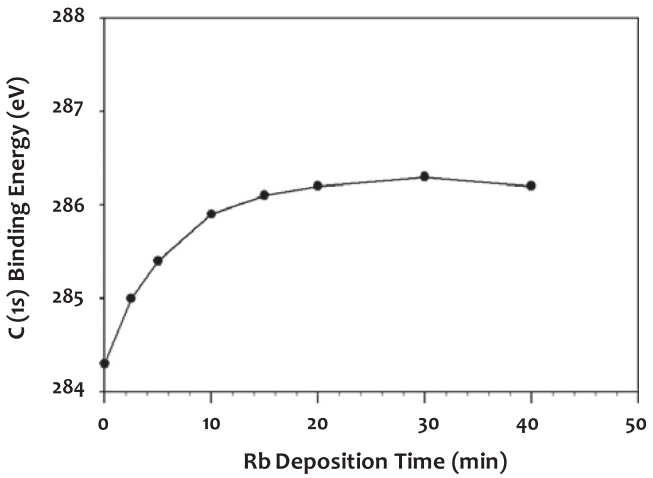

FIG. 4. C1s binding energy (eV) vs. Rb deposition time (min) for a 1-dodecanethiol (DT) monolayer on Au. The C1s position increases rapidly at first and then reaches a maximum (~286.1 eV) and remains at this position for the rest of the 40 min deposition time.

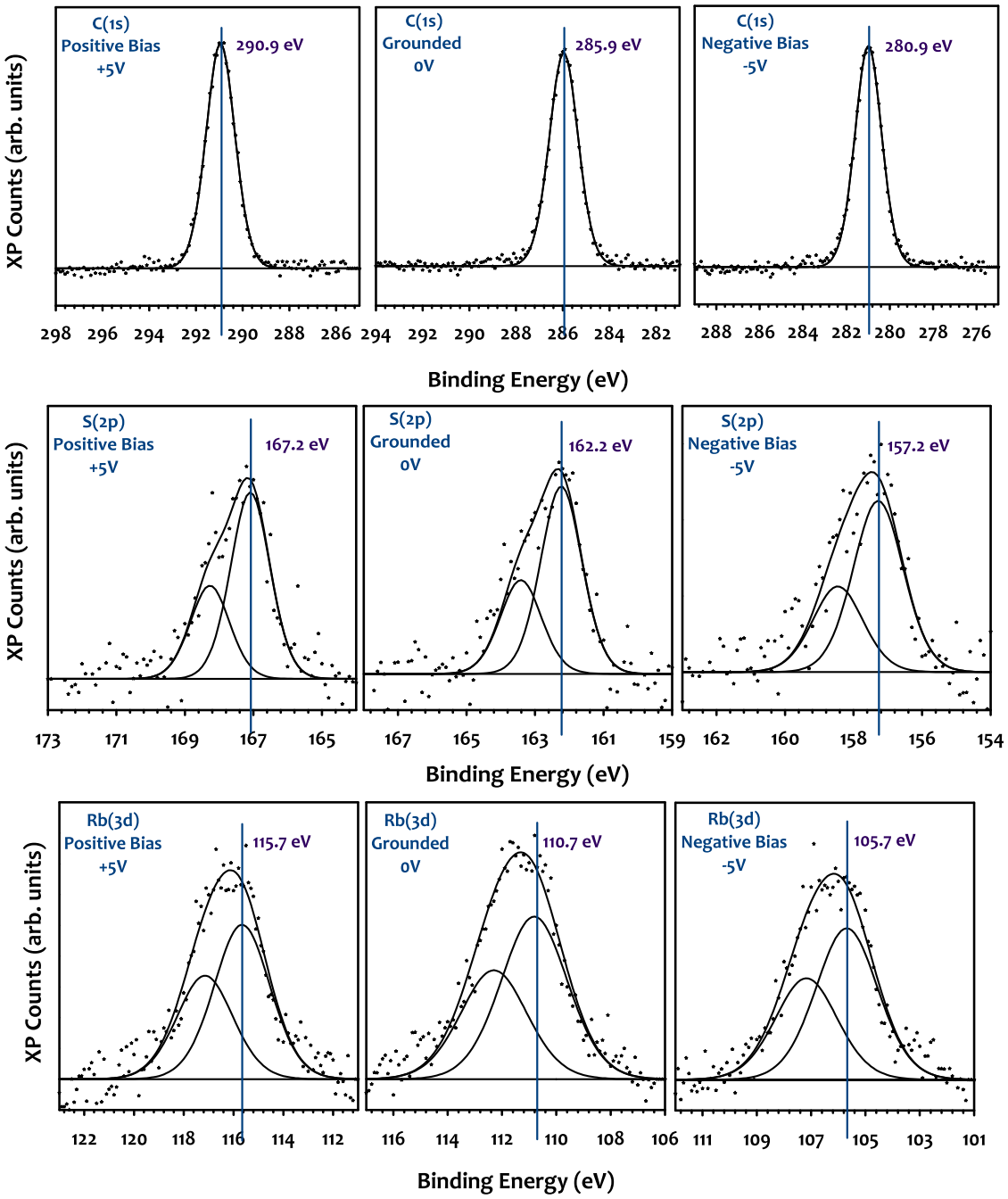

FIG. 5. XPS spectra of a 1-dodecanethiolate (DT) monolayer on Au that has been exposed to Rb vapor. Rb3d, S2p, and C1s spectra were acquired while applying an external dc bias to the sample (±5.0 V). An exactly 10.0 V separation is observed in all regions.

an exactly 10.0 V peak separation is observed for Rb3d, S2p, and C1s core-levels upon application of ±5.0 V biases to the sample. Additionally, no secondary components, which would arise from unequal charge distributions throughout the film, appeared with the applied positive/negative potentials. These results indicate that all species within the film are in unhindered electronic communication, and it can be concluded that no surface charging is occurring with these samples. Thus, we may attribute the observed binding energy shifts as due to Rb interacting with the film. It should be noted that the results of the present study are distinct from a related study by Suzer *et al.*[35] where small charging shifts were observed for an OTS sample exposed to Rb vapor. In our study, the Rb-DT sample was not exposed to ambient conditions prior to analysis, whereas the Rb-OTS sample was handled in air prior to XPS bias studies.

There are numerous reports in the literature of XPS core-level shifts resulting from AM atoms interacting with various films.[49–52] The shifts arise from a transfer of electron density from AM atoms to the surface; this charge transfer may result in an energy increase of the highest energy molecular orbitals, which effectively raises the binding energy.[51,53] Likewise, the higher binding energy shifts reported here are attributed to charge transfer from Rb atoms to the alkanethiolate monolayers. It is concluded that charge transfer does not result in a permanent bonding of Rb to carbon atoms in the SAM. First,

in this case we would expect a lower binding energy carbide-type C1s signal, which is not observed. Second, the C1s peak shifts are essentially reversed and the Rb is oxidized following exposure to air indicating that Rb is not irreversibly bound to carbon. Finally, LIAD experiments have demonstrated the reversible release of AM atoms from hydrocarbon coatings, and we expect alkanethiolates to behave similarly. Thus, an interesting study would be to measure the Rb atomic percent changes that occur with light (or heat); such a study is conducted on a related coating and described in a manuscript to be submitted.[54] The reason why greater shifts are observed (and in some cases are the only shifts observed) for C1s signals than S2p can in part be explained by the close-packing of the films, which results in a higher concentration of Rb atoms in proximity to the alkyl chains than the underlying sulfur head group.

Perhaps the most interesting finding comes from examination of the atomic percent of Rb as Rb is deposited on the film over time. As seen in Figure 6, the amount of Rb on the OT and DT surfaces does not continually increase with increasing deposition time, rather, the Rb concentration increases rapidly at first and then saturates. That is, even with continued exposure to atomic Rb vapor from the dispenser, very little Rb deposits on the surface. This saturation behavior is not altogether surprising considering that a decrease in Rb sticking coefficient is expected with increasing coverage.[55] Thus, once the Rb concentration on the surface reaches a threshold amount, the probability of additional deposition approaches zero. This behavior may have important consequences for magnetometer coatings, as a minimization of interactions between polarized AM atoms and the surface, where depolarizing agents may be present,[8] will suppress spin relaxation. Thus, the high atomic percent of Rb in the SAMs observed here is not expected to create additional relaxation through Rb-Rb collisions, but rather reduce relaxation by possibly decreasing the residence time polarized atoms spend on the AM atom-saturated film. A valuable study would be to measure AM atom residence times as a function of Rb concentration within the film.[8] With regard to LIAD, the curing process may be understood as the time needed to reach the AM atom saturation limit at which point stable vapor densities within the cell are reached. The implications of AM atom saturation on a surface, coupled with the effect of charge transfer, are addressed in an ongoing study focused on currently used atomic vapor cell coatings.[56]

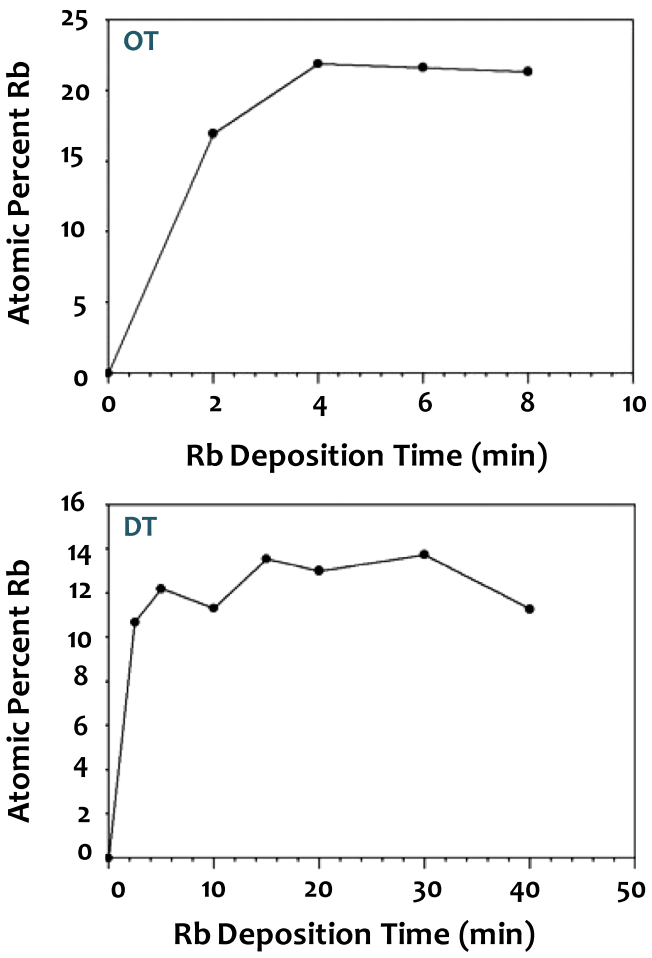

FIG. 6. Atomic percent Rb for 1-octanethiolate (OT) and 1-dodecanthiolate (DT) monolayers on Au as a function of Rb deposition time (min). The concentration of Rb on the monolayer saturates.

CONCLUSIONS

Metallic Rb atoms were deposited on two alkanethiolate SAMs on Au, DT, and OT. Using AR-XPS, Rb was found to intercalate into the film indicating that in atomic vapor cells, AM atoms likely diffuse into wall coatings. Following Rb deposition, shifts of C1s core-level to higher binding energies was observed for all samples. The origin of the shift is attributed to a transfer of electron density from Rb atoms to the monolayer surface. Finally, the atomic percentages of Rb on DT and OT were found to reach a saturation point beyond which little to no additional Rb was deposited on the surface. This behavior is important with regard to vapor cell wall coatings as a Rb-saturated surface may minimize interactions between polarized atoms and wall coatings, thereby preserving spin orientation.

ACKNOWLEDGMENTS

The support of the Office of Naval Research MURI award SA4845-10556 and the Chemistry Division of the National Science Foundation (CHE-0910549) is gratefully acknowledged. We also acknowledge useful discussions with Professor Dmitry Budker.

[1]D. Budker and M. Romalis, Nat. Phys. **3**(4), 227–234 (2007).
[2]Y. Y. Jau, A. B. Post, N. N. Kuzma, A. M. Braun, M. V. Romalis, and W. Happer, Phys. Rev. Lett. **92**(11), 110801 (2004).
[3]A. Kuzmich, L. Mandel, and N. P. Bigelow, Phys. Rev. Lett. **85**(8), 1594 (2000).
[4]B. Julsgaard, J. Sherson, J. I. Cirac, J. Fiurasek, and E. S. Polzik, Nature **432**(7016), 482–486 (2004).
[5]M. V. Balabas, D. Budker, J. Kitching, P. D. D. Schwindt, and J. E. Stalnaker, J. Opt. Soc. Am. B **23**(6), 1001–1006 (2006).
[6]W. Wasilewski, K. Jensen, H. Krauter, J. J. Renema, M. V. Balabas, and E. S. Polzik, Phys. Rev. Lett. **104**(13), 133601 (2010).
[7]E. B. Alexandrov, M. V. Balabas, D. Budker, D. English, D. F. Kimball, C. H. Li, and V. V. Yashchuk, Phys. Rev. A **66**(4), 042903 (2002).
[8]M. A. Bouchiat and J. Brossel, Phys. Rev. **147**(1), 41–54 (1966).
[9]C. Rahman and H. Robinson, IEEE J. Quantum Electron. **23**(4), 452–454 (1987).

[10]Y. W. Yi, H. G. Robinson, S. Knappe, J. E. Maclennan, C. D. Jones, C. Zhu, N. A. Clark, and J. Kitching, J. Appl. Phys. **104**(2), 023534–023537 (2008).
[11]K. F. Zhao, M. Schaden, and Z. Wu, Phys. Rev. A **78**(3), 034901 (2008).
[12]S. J. Seltzer, D. M. Rampulla, S. Rivillon-Amy, Y. J. Chabal, S. L. Bernasek, and M. V. Romalis, J. Appl. Phys. **104**(10), 103116–103117 (2008).
[13]J. C. Camparo, J. Chem. Phys. **86**(3), 1533–1539 (1987).
[14]S. N. Atutov, R. Calabrese, V. Guidi, B. Mai, A. G. Rudavets, E. Scansani, L. Tomassetti, V. Biancalana, A. Burchianti, C. Marinelli, E. Mariotti, L. Moi, and S. Veronesi, Phys. Rev. A **67**(5), 053401 (2003).
[15]W. Hansel, P. Hommelhoff, T. W. Hansch, and J. Reichel, Nature **413**(6855), 498–501 (2001).
[16]J. C. Camparo, R. P. Frueholz, and B. Jaduszliwer, J. Appl. Phys. **62**(2), 676–681 (1987).
[17]X. Zeng, Z. Wu, T. Call, E. Miron, D. Schreiber, and W. Happer, Phys. Rev. A **31**(1), 260–278 (1985).
[18]A. Gozzini, F. Mango, J. H. Xu, G. Alzetta, F. Maccarrone, and R. A. Bernheim, Nuovo Cimento D **15**(5), 709–722 (1993).
[19]S. Gozzini, A. Lucchesini, L. Marmugi, and G. Postorino, Eur. Phys. J. D **47**(1), 1–5 (2008).
[20]A. Cappello, C. de Mauro, A. Bogi, A. Burchianti, S. Di Renzone, A. Khanbekyan, C. Marinelli, E. Mariotti, L. Tomassetti, and L. Moi, J. Chem. Phys. **127**(4), 044706 (2007).
[21]M. T. Graf, D. F. Kimball, S. M. Rochester, K. Kerner, C. Wong, D. Budker, E. B. Alexandrov, M. V. Balabas, and V. V. Yashchuk, Phys. Rev. A **72**(2), 023401 (2005).
[22]C. Marinelli, K. A. Nasyrov, S. Bocci, B. Pieragnoli, A. Burchianti, V. Biancalana, E. Mariotti, S. N. Atutov, and L. Moi, Eur. Phys. J. D **13**(2), 231–235 (2001).
[23]M. Meucci, E. Mariotti, P. Bicchi, C. Marinelli, and L. Moi, Europhys. Lett. **25**(9), 639–643 (1994).
[24]A. Bogi, C. Marinelli, A. Burchianti, E. Mariotti, L. Moi, S. Gozzini, L. Marmugi, and A. Lucchesini, Opt. Lett. **34**(17), 2643–2645 (2009).
[25]H. G. Robinson and C. E. Johnson, Appl. Phys. Lett. **40**(9), 771–773 (1982).
[26]S. J. Seltzer and M. V. Romalis, J. Appl. Phys. **106**(11), 114905 (2009).
[27]D. Budker, L. Hollberg, D. F. Kimball, J. Kitching, S. Pustelny, and V. V. Yashchuk, Phys. Rev. A **71**(1), 012903 (2005).
[28]M. V. Balabas, T. Karaulanov, M. P. Ledbetter, and D. Budker, Phys. Rev. Lett. **105**(7), 070801 (2010).
[29]S. J. Seltzer, P. J. Meares, and M. V. Romalis, Phys. Rev. A **75**(5), 051407 (2007).
[30]S. J. Seltzer, D. J. Michalak, M. H. Donaldson, M. V. Balabas, S. K. Barber, S. L. Bernasek, M. A. Bouchiat, A. Hexemer, A. M. Hibberd, D. F. J. Kimball, C. Jaye, T. Karaulanov, F. A. Narducci, S. A. Rangwala, H. G. Robinson, A. K. Shmakov, D. L. Voronov, V. V. Yashchuk, A. Pines, and D. Budker, J. Chem. Phys. **133**(14), 144703 (2010).
[31]M. W. Tsao, C. L. Hoffmann, J. F. Rabolt, H. E. Johnson, D. G. Castner, C. Erdelen, and H. Ringsdorf, Langmuir **13**(16), 4317–4322 (1997).
[32]T. J. Lenk, V. M. Hallmark, C. L. Hoffmann, J. F. Rabolt, D. G. Castner, C. Erdelen, and H. Ringsdorf, Langmuir **10**(12), 4610–4617 (1994).
[33]A. Ulman, Chem. Rev. **96**(4), 1533–1554 (1996).
[34]S. Suzer, Anal. Chem. **75**(24), 7026–7029 (2003).
[35]S. Suzer, E. Abelev, and S. L. Bernasek, Appl. Surf. Sci. **256**(5), 1296–1298 (2009).
[36]M. Dubey, I. Gouzman, S. L. Bernasek, and J. Schwartz, Langmuir **22**(10), 4649–4653 (2006).
[37]J. Gorham, B. Smith, and D. H. Fairbrother, J. Phys. Chem. C **111**(1), 374–382 (2006).
[38]P. E. Laibinis and G. M. Whitesides, J. Am. Chem. Soc. **114**(6), 1990–1995 (1992).
[39]T. Seto, T. Hara, and K. Tanaka, Jpn. J. Appl. Phys., Part 1 **7**(1), 31–42 (1968).
[40]J. Hrbek, G. Q. Xu, T. K. Sham, and M. L. Shek, J. Vac. Sci. Technol. A **7**(3), 2013–2015 (1989).
[41]G. Ebbinghaus and A. Simon, Chem. Phys. **43**(1), 117–133 (1979).
[42]B. N. J. Persson and H. Ishida, Phys. Rev. B **42**(5), 3171–3174 (1990).
[43]X. Shi, D. Tang, D. Heskett, K. D. Tsuei, H. Ishida, and Y. Morikawa, Surf. Sci. **290**(1–2), 69–79 (1993).
[44]X. Shi, D. Tang, D. Heskett, K. D. Tsuei, H. Ishida, Y. Morikawa, and K. Terakura, Phys. Rev. B **47**(7), 4014–4017 (1993).
[45]T. K. Sham, M. L. Shek, G. Q. Xu, and J. Hrbek, J. Vac. Sci. Technol. A **7**(3), 2191–2193 (1989).
[46]G. F. Meyers, M. B. Hall, J. W. Chinn, and R. J. Lagow, J. Am. Chem. Soc. **107**(5), 1413–1414 (1985).
[47]L. Ramqvist, K. Hamrin, G. Johansson, A. Fahlman, and C. Nordling, J. Phys. Chem. Solids **30**(7), 1835–1847 (1969).
[48]I. N. Shabanova and V. A. Trapeznikov, J. Electron. Spectrosc. **6**(4), 297–307 (1975).
[49]H. Estradeszwarckopf and B. Rousseau, J. Phys. Chem. Solids **53**(3), 419–436 (1992).
[50]B. Rousseau and H. Estradeszwarckopf, Solid State Commun. **85**(9), 793–797 (1993).
[51]S. P. Kelty, Z. Lu, and C. M. Lieber, J. Phys. Chem. **95**(18), 6754–6756 (1991).
[52]S. J. Weyers, O. Janzen, and W. Monch, J. Phys. Condens. Matter **11**(43), 8489–8494 (1999).
[53]M. S. Dresselhaus and G. Dresselhaus, Adv. Phys. **30**(2), 139–326 (1981).
[54]A. M. Hibberd, S. J. Seltzer, M. Morse, M. V. Balabas, D. Budker, and S. L. Bernasek, "Synchrotron radiation x-ray photoelectron spectroscopy depth-profiling study of light induced atomic desorption," (unpublished).
[55]G. A. Somorjai, *Introduction to Surface Chemistry and Catalysis* (John Wiley & Sons, New York, 1994).
[56]A. M. Hibberd, M. Balabas, S. J. Seltzer, D. Budker, and S. L. Bernasek, "Synchrotron radiation x-ray photoelectron spectroscopy study of alkene-based atomic vapor cell coatings," (unpublished).